SIMULATION OF 1-MINUTE POWER OUTPUT FROM UTILITY-SCALE PHOTOVOLTAIC GENERATION SYSTEMS

Joshua S. Stein
Sandia National Laboratories
P.O. Box 5800 MS 1033
Albuquerque, NM 87185
e-mail: jsstein@sandia.gov

Clifford W. Hansen
Sandia National Laboratories
P.O. Box 5800 MS 1033
Albuquerque, NM 87185
e-mail: cwhanse@sandia.gov

Abraham Ellis
Sandia National Laboratories
P.O. Box 5800 MS 1033
Albuquerque, NM 87185
e-mail: aellis@sandia.gov

Vladimir Chadliev
NV Energy
6226 W. Sahara Ave.
Las Vegas, NV 89146
e-mail: vchadliev@nvenergy.com

ABSTRACT

Sandia National Laboratories has developed a modeling approach to simulate time-synchronized, 1-minute power output from large PV plants in locations where only hourly irradiance measurements are available via satellite sources. The approach uses 1-min irradiance measurements from analogue sites in a similar geographic area. PV output datasets generated for 2007 in southern Nevada are being used for a Solar PV Grid Integration Study to estimate the integration costs associated with various utility-scale PV generation levels. Plant designs considered include both fixed-tilt thin-film, and single-axis-tracked polycrystalline Si systems ranging in size from 5 to 300 MW_{AC}. Simulated power output profiles at 1-min intervals were generated for five scenarios (149.5 MW, 222 WM, 292 MW, 492 MW, and 892 MW) each comprising as many as 10 geographically separated PV plants.

1. INTRODUCTION

NV Energy balances load and generation for most of the state of Nevada and is studying how different levels of photovoltaic (PV) generation will affect load balancing for the utility. Sandia National Laboratories (SNL) participated in this study by producing time-synchronized, 1-min PV output profiles for proposed PV plants at 10 locations across southern Nevada (Fig 1) for 2007 (last highest summer peak load year for the utility). NV Energy and its consultant, Navigant Consulting, will use these profiles to calculate the effect on balancing operations (e.g., additional load following and regulation reserves) of various levels of utility-scale PV generation.

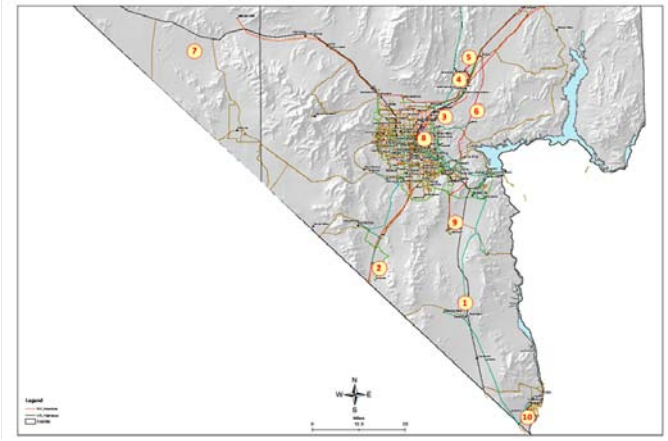

Fig. 1. Map of ten PV sites considered in the study.

2. MODEL DESCRIPTION

The instantaneous power output from a PV plant is determined by a number of factors, including: module and inverter characteristics; irradiance over the plant area; temperature of the PV cells; angle of incidence and spectral quality of the light; and losses, including soiling, wiring, and conversion losses.

Based on many years of outdoor module and array testing, Sandia has developed the Sandia PV Array Performance Model [1]. One challenge of applying this and other PV performance models to large PV systems is that the models generally expect a single value of irradiance as input. As PV systems become larger it is more likely that irradiance will vary spatially over the plant as cloud

shadows pass over parts of the plant's footprint.

2.1 Spatial Average of Irradiance

Studies performed by Sandia at the La Ola 1.2 MW PV plant in Lanai, HI [2] have focused on understanding the relationship between plant output and irradiance measured by a network of irradiance sensors spread over the plant footprint. This study has shown that short-term (1-sec) power output from a PV plant is approximately proportional to the spatial average of plane of array (POA) irradiance over the plant footprint. Figure 2 shows a scatterplot of 1-sec AC power from the plant against POA irradiance from a single sensor within the plant and the spatial average of POA irradiance determined from 16 sensors distributed within the plant area. It is apparent from the figure that the spatial average of POA irradiance is much better correlated with the power output than irradiance from a single sensor. The yellow dotted line shows the fit for a reference clear day. The fact that this relationship is very similar for both clear and partly cloudy days implies that the spatial average of irradiance can be used in the PV performance model to predict power for all conditions. The modeling approach described in the next sections aims to first simulate 1-min point irradiance at locations without ground-based measurements, and then to estimate the spatial average irradiance over the area of the PV plant being considered. This average is then used as input to the performance model.

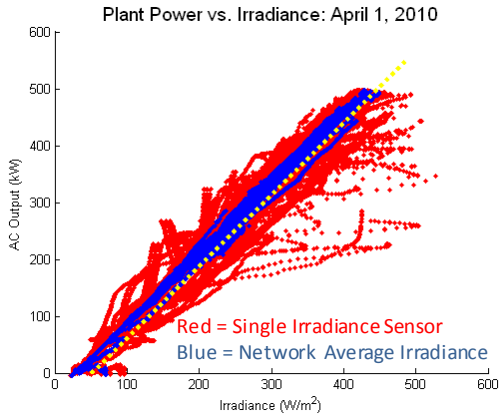

Fig. 2. Relationship between irradiance and AC power from the entire plant for April 1, 2010, a partly cloudy day.

2.2 Estimation of 1-min Point Irradiance at Study Sites

One-minute averages of global horizontal irradiance are available at six Las Vegas Valley Water District (LVVWD) PV installations within the Las Vegas valley as shown in Table 1. No ground-based data is available at the 10 sites identified by NV Energy for the study so we developed a method to simulate 1-min irradiance for each of these 10 sites.

TABLE 1. IRRADIANCE MEASURMENT GROUND STATIONS

Station Name	Start Date for Data
Fort Apache	8/23/2006
Grand Canyon	9/30/2006
Las Vegas State Park	7/26/2007
Spring Mountain	11/30/2006
LUCE	5/2/2007
Ronzone	4/27/2006

Estimates of irradiance at hourly intervals on a 10×10 km grid for the United States are available through the SolarAnywhere service from Clean Power Research [3]. This data is currently provided free of charge for time periods older than 3 years. Irradiance is estimated from GOES satellite imagery using algorithms developed by Perez and others [4]. These algorithms have been validated by several researchers [5-7]. Irradiance estimates at hourly intervals for the 10 study sites were obtained. These estimates represent instantaneous irradiance over a single satellite pixel (~1 km^2), which is somewhere in the 10×10 km area. Errors on the geopositioning of pixels can be as great as several kilometers between images. These data were used to calculate hourly average irradiance by averaging the two measurements which span the hour (the start and end of the hour).

To estimate 1-min irradiance at each site, we considered several options. First we reviewed a number of irradiance simulation models which aim to simulate time series of irradiance. These models generally work with clearness index (irradiance divided by clear sky irradiance), which is generally characterized as a bimodal distribution when the time intervals are short (e.g., 1-min). Skartveit and Olseth [8] proposed a method to estimate this distribution shape based on hourly average irradiance and interhour variability. To simulate a time series of irradiance, they proposed to sample from the distribution and then reorder the sampled clearness values to achieve a target lag one autocorrelation. Tovar and others [9-12] have identified alternative relationships between the frequency distribution of clearness index and quantities such as the air mass and hourly average irradiance but do not specify a method for simulating time series. An approach suggested by Glasbey [13] involves simulating clearness index as a nonlinear autoregressive time series with the

joint distributions of clearness at lag 1 defined by multivariate Gaussian mixtures. After fitting these models to data from the Las Vegas valley and simulating 1-min irradiance time series, we found that the variance in the simulated irradiance was generally higher than observed in the ground-based irradiance measurements. We attribute the higher variance to the low lag considered in the fitted models. Use of these models would result in more frequent or larger ramps in simulated power than are supported by available data.

Therefore we decided to develop an approach that produced 1-min irradiance time series that closely match the hourly averages and honor any seasonal patterns that might exist. Our method starts by assembling a library of more than 5,000 one-day sequences of irradiance at 1-min intervals using all available ground station data (Table 1). We calculated the hourly average irradiance for each day in the library. Next, for each day at each of the 10 study sites, we calculated the sum of the squared differences (SSE) between the hourly averaged target irradiance (from the satellite) and the hourly average of irradiance for each of the library days. We then sorted the library days and kept track of the 10 library days with the lowest SSE (best fit) for each day of 2007 and at each site.

The next step involved assigning a library irradiance day (1-min data) to each site for each day of the year. To prevent the same library day being assigned to more than one site for each day of the year, we generated a random permutation of 1 to 10 for each day of the year. These samples represent the order in which we assign library days to the sites. For example, if the first four integers are 4, 1, 9, 2, … for a particular day, we start at Site 4 and choose the library day with the lowest SSE for that site and day. Next we examine Site 1. If the library day chosen for Site 4 also has the lowest SSE for Site 1, we choose the library day for Site 1 that has the second lowest SSE. We consider the remaining sites in the permutation order (9, 2, …) until library days are assigned for each site. Then we proceed to the next day of the year and repeat the procedure. The permutation process ensures that the selection algorithm does not produce perfectly-correlated 1-min irradiance at different sites on the same day. Figure 3 shows an example of the satellite irradiance for a day and the 1-min irradiance day from the library that was chosen.

The ground-based measurements of irradiance used to assign irradiance days to each plant location represent point measurements rather than spatial averages. The next step is to estimate the spatial average irradiance over each plant footprint. For this study we considered five scenarios (149.5 MW, 222 WM, 292 MW, 492 MW, and 892 MW). Each of these scenarios was defined as a mix of PV plants of varying sizes at each of the 10 sites (Table 2).

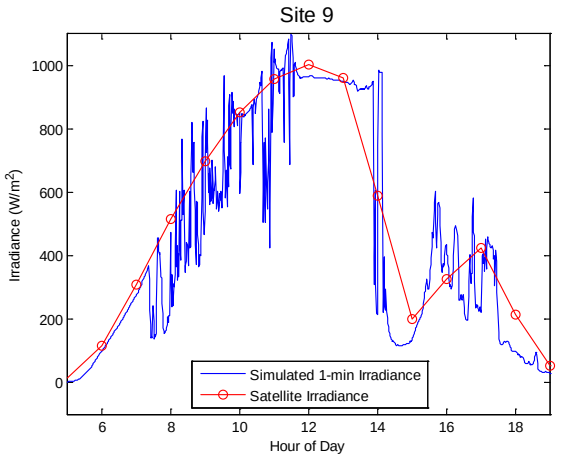

Fig. 3. Comparison of satellite (red) and the best fit 1-min irradiance day.

2.3 Estimation of Spatially Averaged Irradiance at Study Sites

TABLE 2. PV PLANT SIZES (MW_{AC}) FOR EACH SCENARIO

	Scenario				
Site	**S1**	**S2**	**S3**	**S4**	**S5**
1	17.5	20	20	20	20
2*	50	50	100	100	300
3*	12	27	27	27	27
4	40	40	60	60	60
5*	-	50	50	100	200
6	30	30	30	30	30
7	-	-	-	50	100
8*	-	5	5	5	5
9*	-	-	-	50	100
10	-	-	-	50	50
Scenario Total (MW_{AC})	149.5	222	292	492	892
	* These PV plants are specified to be latitude tilt, thin-film modules. Other plants are specified to be single axis tracking, polycrystalline Si modules				

Given a plant size (in MW_{AC}) and a technology (polycrystalline Si or thin-film), we made assumptions to estimate the land area required (Table 3).

For each plant listed in Table 2, we calculate PV plant area as the product of the plant capacity (MW_{AC}) and the conversion factor (acres/MW_{AC}) from Table 3, depending on the plant type.

TABLE 3. PV SYSTEM DESCRIPTIONS

Module Technology	Mounting Configuration	Land Requirements (acres/MW_{AC})
Polycrystalline Si	Single-axis tracking	10
Thin-Film	Fixed latitude tilt	12.5

To estimate the spatial average irradiance over each plant we apply the methodology developed by Longetto et al. [14]. This method assumes that the spatial average of irradiance over an area can be estimated as a time average of point measurements of irradiance with an averaging window equal to the time it takes for a cloud to pass over the array. To apply this method we need to know the characteristic length of the plant and the velocity of the cloud shadows across the landscape. The characteristic length of the plant was estimated as the square root of the plant area (i.e., we assume plants are square). The cloud velocity was estimated from upper air wind speed measurements made by NOAA from weather balloons launched from the Desert Rock station in Mercury, NV [15]. These balloons are launched every 12 hours throughout the year. To estimate wind speed at cloud level we calculated the average of the wind speeds measured within the altitude interval from 1,000 to 8,000 meters above sea level. Figure 4 shows the distribution of resulting upper air wind speeds for 2007 (mean = 6.2 m/s).

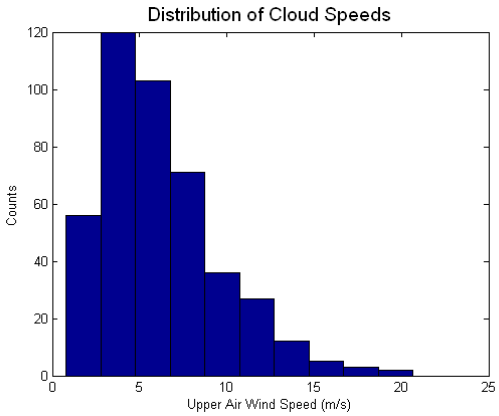

Fig. 4. Distribution of calculated upper air wind speed from Desert Rock station for 2007.

Figure 5 illustrates the effect of plant size on reducing the variability of irradiance by averaging over plant area. Greater reduction in variability is to be expected as plants become larger, due to the longer time required for cloud shadows to pass over the plant.

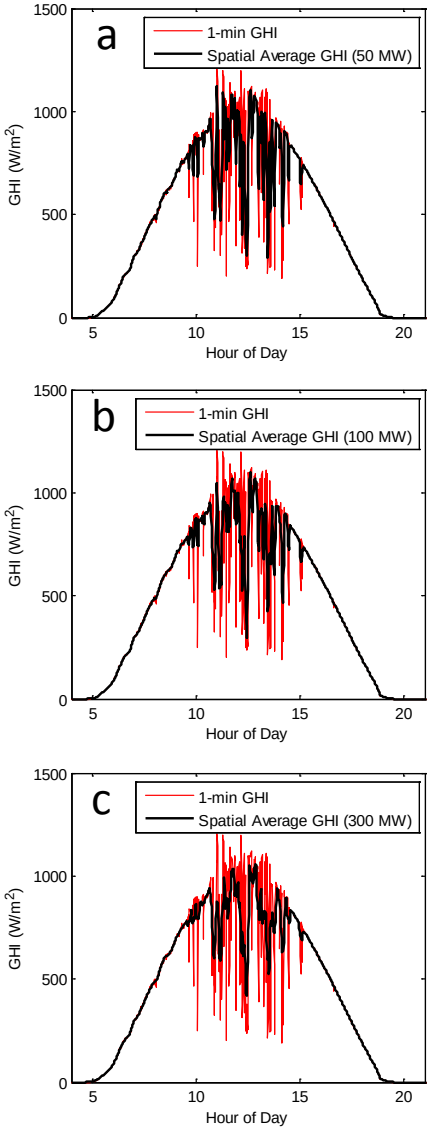

Fig. 5. Comparison of 1-min point irradiance and estimated spatial average irradiance for three different plant sizes: 50 MW (a), 100 MW (b), and 300 MW (c).

2.4 Translation to Plane-of-Array Irradiance at Study Sites

To apply the Sandia PV Array Performance Model [1] we need to calculate the direct and diffuse components of POA irradiance. We applied the DISC model [16] to estimate the direct normal irradiance (DNI) from the GHI and calculated the diffuse (horizontal) as the difference: GHI - DNI × cos(Z), where Z is the zenith angle. The

DISC model is based on empirical data collected across the U.S. relating the diffuse fraction to GHI. Beam irradiance at the POA is DNI × cos(AOI), where AOI is the angle of incidence between the sun and the module surface. The AOI is calculated from Eq 1:

$$AOI = \cos^{-1}\left[\begin{array}{c}\cos(Z)\cos(T_a)+\\ \sin(Z)\sin(T_a\cos(A_s - A_a)\end{array}\right], \quad (1)$$

where Z is the solar zenith angle, T_a is the tilt angle of the array, A_s is the solar azimuth angle (0°=North, 90°= East), and A_a is the array azimuth angle (0°=North, 90°= East).

In the case of the fixed (thin-film) arrays, AOI is simply a function of the solar zenith and azimuth angles, which vary with time. For single-axis tracked system (where the tracking axis is horizontal and oriented N-S), the tilt angle, array azimuth, and solar zenith angle vary with time. Eqs. 2 to 5 describe the calculation of the array tilt and azimuth angles, T_a and A_a for this configuration [17]:

$$\alpha = -\tan^{-1}\left[\frac{-\sin(Z)\sin(A_s)}{\cos(Z)}\right] \quad (2)$$

$$\beta = \left\{\begin{array}{c}T_m\\ -T_m\\ \alpha\end{array}\right\} if \left\{\begin{array}{c}\alpha > T_m\\ \alpha < -T_m\\ else\end{array}\right\} \quad (3)$$

where T_m is the maximum tilt angle for the tracker (assumed to be 45°).

$$T_a = |\beta| \quad (4)$$

$$A_a = \left\{\begin{array}{c}90°\\ 270°\end{array}\right\} if \left\{\begin{array}{c}\beta >= 0\\ \beta < 0\end{array}\right\} \quad (5)$$

Diffuse irradiance on the POA was calculated using the translation model developed by Perez et al. [18]. The ground reflectance was assumed to be constant (0.2). It is assumed that there is no shading of the array.

2.5 Calculation of 1-min AC Power Output at Study Sites

DC power output from each array was estimated using the Sandia PV Array Performance Model [1] to calculate the maximum power point for each minute of the year. AC power was determined using the Sandia PV Inverter Model [19]. We assumed that the polycrystalline Si plants use Yingli Solar YL230-29b modules and that thin film plants use First Solar FS-275 modules. Both types of plants were assumed to be divided into 500 kW_{AC} blocks and use SatCon PVS-500 ($480V_{AC}$) inverters. These technology assumptions were necessary in order to run the models but are not likely to affect the model results in a significant way, because the differences between similar modules are relatively small in comparison to the magnitude of the variability in irradiance. A sufficient number of series strings were used so that the product of the assumed DC derate factor of 0.85 and the DC rating of the modules was equal to the AC rating of the system (in MW).

Cell temperature was estimated using the King model [1], which includes the effects of POA irradiance, air temperature and wind speed. Weather data were used from 2007 in Las Vegas; measured wind speed at McCarran International airport was used for each site, while measured air temperature data was lapse-adjusted for elevation differences between each site and the airport meteorological station.

3.0 RESULTS

One-minute annual estimates of AC power output were produced for each plant listed in Table 2. Figure 6 shows an example of the output profiles from a clear day for all plants included in Scenario S1. Note the different shapes for fixed-tilt and single axis tracked systems. Figure 7 shows profiles for a partly cloudy day for Scenarios S1 and S4. Note that the output profiles are different for each scenario because the number and size of plants between scenarios.

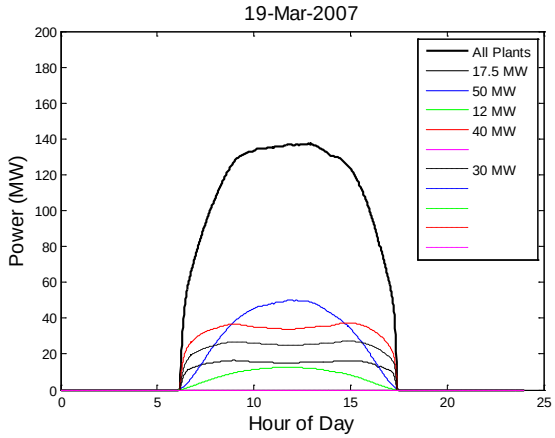

Fig. 6. Example simulated AC power output profiles for Scenario S1 for a clear day.

4. MODEL VALIDATION

Validation of this modeling approach is challenging because performance data from utility-scale PV systems that exist at locations where we simulate performance is

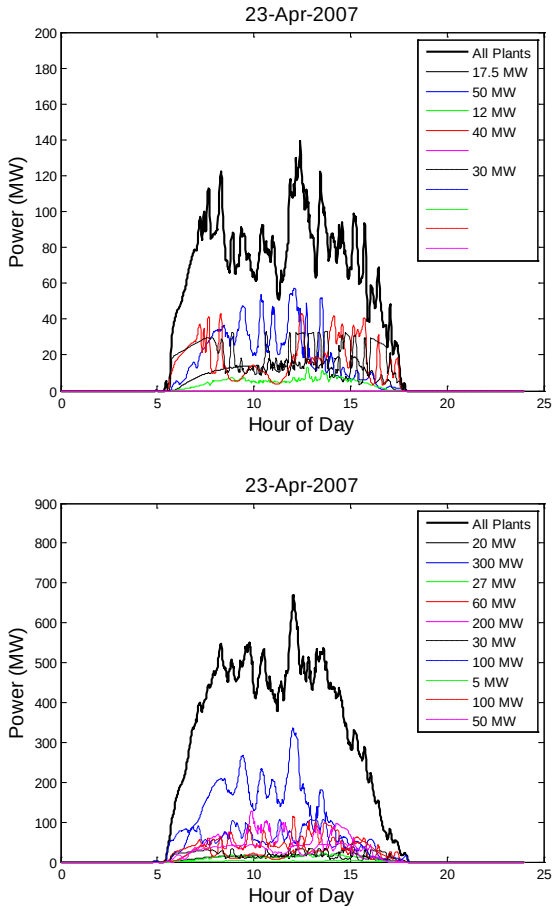

Fig. 7. Example AC power output profiles for a partly cloudy day for Scenario S1 (top) and Scenario S5 (bottom).

proprietary and moreover, many of the PV plants we simulate are significantly larger than any PV plant yet built anywhere in the world. Therefore, our validation efforts at this stage are focused on comparisons between simulated irradiance and power output, and what we know to be general patterns and relationships of irradiance measured at different locations in the field. Future work is underway to test this modeling approach directly by simulating performance of existing large PV plants and making comparisons with measured plant output but such comparisons are not ready to be reported here.

Model validation at this stage is demonstrated by comparing:
(1) distributions of simulated 1-min irradiance and satellite measured irradiance;
(2) distributions of simulated irradiance changes and measured irradiance changes from the LVVWD sites;
(3) correlation coefficients for changes in the clearness index as a function of time;
(4) simulated power changes for a 20 MW plant over 1-min and 10-min intervals.

Figure 8 compares the distributions (cumulative distribution function (CDF) of irradiance measured by satellite (hourly) and simulated irradiance for one of the sites. The nearly identical nature of the distributions indicates that the method used to match irradiance days to satellite data results in an appropriate annual distribution of irradiance at the study sites. These results are repeated at all sites, but not show here.

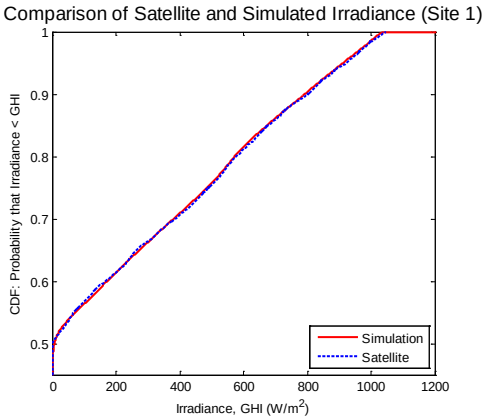

Fig. 8. Comparison between distributions of simulated 1-min irradiance and 1-hour satellite irradiance (Site 1).

Figure 9 compares CDFs of 1-min changes in irradiance between measured ground data from the LVVWD stations (operating in 2007) and simulated irradiance at one of the study sites. The close match between these distributions demonstrates that the model is able to appropriately reproduce the frequency of 1-min changes that are measured in Las Vegas.

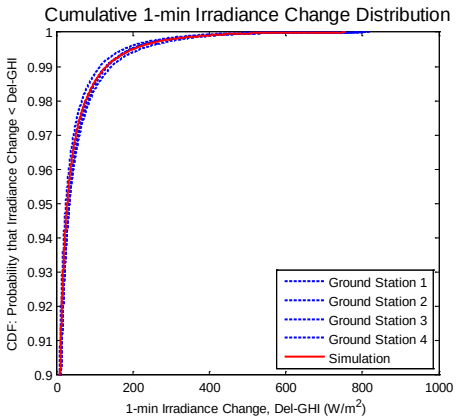

Fig. 9. Comparison between cumulative distributions of simulated 1-min irradiance changes and measured irradiance changes from four LVVWD ground stations.

Mills et al [20] showed that the correlation coefficient of

step changes in the clearness index varied both as a function of separation distance between sites and with the time lag considered. Figure 10 (from [20] shows this relationship for irradiance data collected in the Great Plains. Figure 11 shows the same plot for simulated irradiance generated for the NV Energy study. The similarity between the plots indicates that the simulated irradiance shares certain characteristics with the data measured in the Great Plains. Specifically, correlations between sites decrease with separation distance and increase with the time lag. Correlations are somewhat lower for the simulated data, which might reflect a systematic feature of the model approach, or may be a real difference between weather patterns at the two locations (Great Plains vs. Nevada).

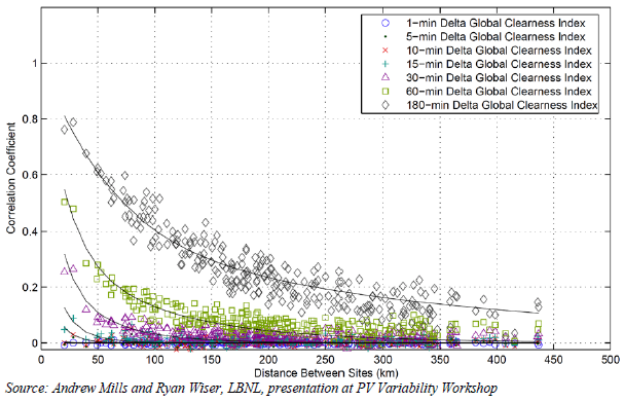

Source: Andrew Mills and Ryan Wiser, LBNL, presentation at PV Variability Workshop

Fig. 10. Correlation patterns for irradiance step changes measured in the Great Plains [20].

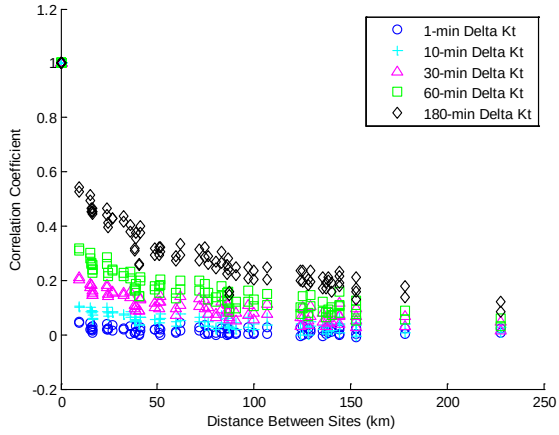

Fig. 11. Correlations between changes in the *simulated* clearness index over various time intervals as a function of distance between ground stations.

However, figure 12 shows the same plot for measured clearness at the six LVVWD sites. Note that the separation distances are smaller than in either figure 10 or figure 11, but the correlation coefficients at the largest separation distance (~12 km) match up very closely with the values at the minimum separation distance in figure 11. This match between measured and simulated datasets suggests that the simulated data is reasonable and that the difference between Nevada and the Great Plains likely reflects differences in weather patterns between the two locations.

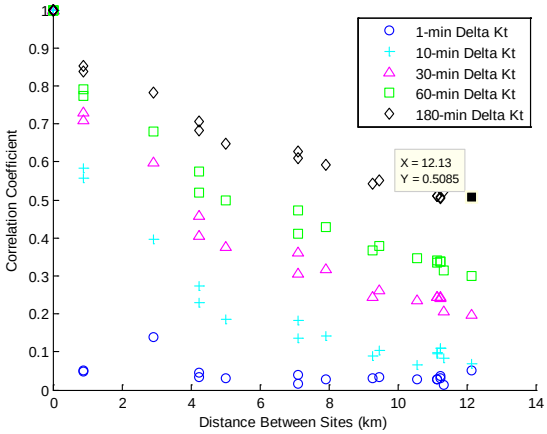

Fig. 12. Correlations between changes in the *measured* clearness index at 6 LVVWD sites over various time intervals as a function of distance between ground stations.

Finally, figure 13 compares the distributions of simulated power ramps for a 20 MW plant as a function of time interval (1 and 10 min). The pattern exhibited (larger ramps for larger time intervals) is very similar to that observed for actual utility scale PV systems of similar size at other locations [20].

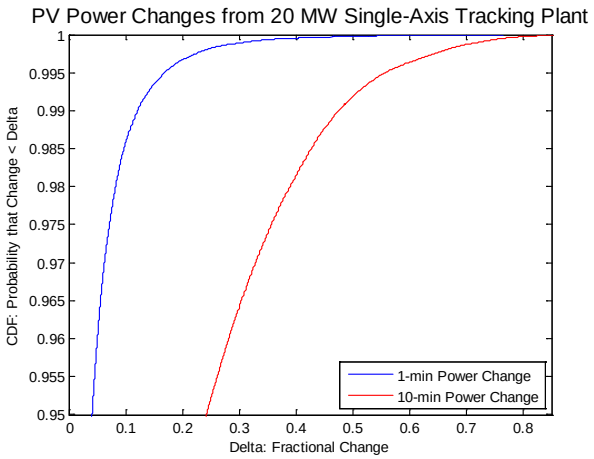

Fig. 13. Cumulative distribution functions (p=0.95 to 1) of 1-min and 10-min power changes from a simulated 20 MW PV plant.

7. SUMMARY AND CONCLUSIONS

We describe a method for simulating 1-min PV output from a set of utility-scale PV plants in southern Nevada, illustrate results obtained using the method, and present evidence supporting the conclusion that the method produces reasonable results. Simulated datasets obtained by this method are being used in a study to estimate the integration costs of different levels of PV generation on the NV Energy system.

8. FUTURE WORK

Follow-on work will focus on further validation of the method by comparing simulated power output to measured power at a large PV plant. We also intend to investigate how this method may be extended so that power may be simulated at locations where few or no ground-based measurements of 1-min irradiance are available.

9. ACKNOWLEDGMENTS

Sandia is a multiprogram laboratory operated by Sandia Corporation, a Lockheed Martin Company, for the United States Department of Energy's National Nuclear Security Administration under contract DE-AC04-94AL85000.

10. REFERENCES

(1) King, D. L., E. E. Boyson, et al., Photovoltaic Array Performance Model, Albuquerque, NM, Sandia National Laboratories. SAND2004-3535, 2004

(2) Kuszmaul, S., A. Ellis, et al., Lanai High-Density Irradiance Sensor Network for Characterizing Solar Resource Variability of MW-Scale PV System. 35th IEEE PVSC, Honolulu, HI, 2010

(3) Clean Power Research SolarAnywhere website: https://www.solaranywhere.com

(4) Perez, R., Ineichen, P., Moore, K., Kmiecik, M., Chain, C., George, R., and Vignola, F, A New Operational Satellite-to-Irradiance Model, Solar Energy 73, 5, pp.307-317, 2002

(5) Stein, J., R. Perez, et al.,, Validation of PV Performance Models using Satellite-Based Irradiance Measurements: A Case Study. SOLAR2010, Phoenix, AZ, 2010

(6) Perez, R., J. Schlemmer, et al., Validation of the SUNY Satellite Model in a Meteosat Environment. Proc., ASES Annual Conference, Buffalo, NY, 2009

(7) Stackhouse, P., T. Zhang, et al., Satellite Based Assessment of the NSRDB Site Irradiances and Time Series from NASA and SUNY/Albany Algorithms. Proc. ASES Annual Meeting, San Diego, CA, 2008

(8) Skartveit, A. and J. A. Olseth, "The probability density and autocorrelation of short-term global and beam irradiance." Solar Energy 49(6): 477-487, 1992

(9) Tovar, J., F. J. Olmo, et al., "One-minute global Irradiance probability density distributions conditioned to the optical air mass." Solar Energy 62(6): 387-393, 1998

(10) Tovar, J., F. J. Olmo, et al., "One-minute kb and kd probability density distributions conditioned to the optical air mass." Solar Energy 65(5): 297-304, 1999

(11) Tovar, J., F. J. Olmo, et al., "Dependence of one-minute global irradiance probability density distributions on hourly irradiation." Energy 26: 659-668, 2001

(12) Tovar-Pescador, J., Modelling the Statistical Properties of Solar, Radiation and Proposal of a Technique Based on Boltzmann Statistics, Modeling Solar Radiation at the Earth's Surface: Recent Advances. V. Badescu. Berlin, Springer-Verlag: 55-91, 2008

(13) Glasbey, C. A., "Nonlinear autoregressive time series with multivariate Gaussian mixtures as marginal distributions." Applied Statistics 50: 143-154, 2001

(14) Longhetto, A., G. Elisei, et al., "Effect of correlations in time and spatial extent on performance of very large solar conversion systems." Solar Energy 43(2): 77-84, 1989

(15) Data obtained from University of Wyoming College of Engineering web service: http://weather.uwyo.edu/upperair/sounding.html Desert Rock station number is 72387.

(16) Maxwell, E. L., A Quasi-Physical Model for Converting Hourly Global Horizontal to Direct Normal Insolation. Golden, CO, Solar Energy Research Institute, 1987

(17) Chang, T. P., "The gain of single-axis tracked panel according to extraterrestrial radiation." Applied Energy 86: 1074-1079, 2009

(18) Perez, Richard; Ineichen, Pierre; and Seals, Robert, Modeling Daylight Availability and Irradiance Components from Direct and Global Irradiance, Solar Energy 44 (5): 271-289, 1990

(19) King, D. l., S. Gonzalez, et al., Performance Model for Grid-Connected Photovoltaic Inverters, Albuquerque, NM, Sandia National Laboratories. SAND2007-5036, 2007

(20) Mills, A., M. Ahlstrom, et al., Understanding Variability and Uncertainty of Photovoltaics for Integration with the Electric Power System, Berkeley National Laboratory. LBNL-2855E, 2009